Available online at www.sciencedirect.com
SCIENCE DIRECT
Journal of Molecular Catalysis A: Chemical 245 (2006) 17–25
JOURNAL OF MOLECULAR CATALYSIS A: CHEMICAL
www.elsevier.com/locate/molcata

Photo-degradation catalyst screening by high throughput experiments

Hai Yuan Xiao [a], Qi Xiu Dai [a], Wen Sheng Li [a], C.T. Au [a,b], Xiao Ping Zhou [a,*]

[a] *Department of Chemical Engineering, Hunan University, 410082 China*
[b] *Department of Chemistry and Centre for Surface Analysis and Research, Hong Kong Baptist University, Kowloon Tong, Hong Kong*

Received 22 March 2005; received in revised form 17 September 2005; accepted 17 September 2005
Available online 21 October 2005

Abstract

A high throughput fluorescence photo-imaging method has been developed for the screening of photo-degradation catalysts. When employed to analyze the photo-degradation of 1,6-hexamethylenediamine (the probe molecule), the method produced results that are comparable to that when methyl orange was employed as a probe molecule and UV spectrometry as an analysis device. We found that the variation trends in catalytic activity over the same group of catalysts are the same in both cases. The results indicate that the fluorescence photo-imaging method is applicable to the screening of photo-degradation catalysts. For comparison, mesoporous catalysts of high specific surface area prepared by using P123 ($HO(CH_2CH_2O)_{20}(CH_2CH(CH_3)O)_{70}(CH_2CH_2O)_{20}H$) as a template and "regular" catalysts (those prepared without P123) were tested. The results showed that most of the former catalysts are superior to the latter counterparts. Our study also revealed that the addition of ZrO_2 to TiO_2 did not result in significant improvement in catalytic activities, whereas marked improvement was observed when Nb_2O_5 or WO_3 was added to TiO_2. When Nb_2O_5 and WO_3 were co-doped to TiO_2, the tertiary catalysts exhibited higher catalytic activities. The catalysts containing 20–30% of Nb_2O_5 and 10–20% of WO_3 (balanced with TiO_2) are superior to any of pure TiO_2, Nb_2O_5, WO_3, and the binary catalysts composed of any two of TiO_2, Nb_2O_5, and WO_3. Our study has demonstrated that besides the traditional TiO_2-domain catalysts, active photo-degradation catalysts can be prepared by combination of Nb_2O_5, WO_3, and ZrO_2.

Keywords: Photo-degradation catalysts; High throughput methodology; TiO_2; Nb_2O_5; WO_3

1. Introduction

Photocatalytic oxidation has been proven to be an efficient approach to the removal of organic contaminants in water and air [1]. Light irradiation on semiconductor materials can create electron–hole pairs. The holes are powerful oxidation sites and can oxidize most of the known organic pollutants. In this aspect, TiO_2 and TiO_2 materials doped with metal ions were reported to be active catalysts [2,3]. The catalytic activities of the materials are dependent on factors, such as (i) composition, (ii) size of micro-crystals, (iii) lattice structure, (iv) surface acidity, and (v) surface area. Generally speaking, doping TiO_2 with metal ions could change the nature of the TiO_2 band gap, and hence changing the catalytic activity and light-sensitivity of TiO_2 [4]. In recent years, the deployment of nano-materials has offered opportunities of generating new photo-degradation catalysts. It has been reported that TiO_2 nanocrystals are more active than the commercial P25 (Degussa) [5–8]. Detailed investigation in this area showed that the lattice structure of the materials is a crucial factor in photo-degradation reactions. Berry and Mueller found that at TiO_2 phase composition of anatase/rutile = 70%/30%, the catalyst was more active [9] than either of the pure-phase (anatase or rutile) compound. Wang and co-workers reported that ultra-fine $TiO_2{\cdot}nH_2O$ of anatase phase was responsible for photo-degradation [10]. Besides, surface acidity and specific surface area of catalyst can exert great influence on performance. Generally speaking, materials of high specific surface area have high activity for photo-degradation, and catalysts with acidic surface favor the adsorption of anionic pollutants [11]. Among the influencing factors, catalyst composition and specific surface area are the most important ones because lattice structure, surface acidity, and phase composition of catalysts are usually related with catalyst composition, while porosity, crystal, and particle size with specific surface area. If one could link catalytic property with catalyst composition and specific surface area during primary screening of catalysts, the extent of labor

* Corresponding author. Tel.: +86 7318821017; fax: +86 7318821017.
E-mail address: hgx2002@hnu.cn (X.P. Zhou).

1381-1169/$ – see front matter © 2005 Elsevier B.V. All rights reserved.
doi:10.1016/j.molcata.2005.09.027

work could be reduced. With the identification of promising catalysts, the influence of the other factors could be determined in details in secondary screening or scale-up processes. Up until now, despite extensive studies on photocatalytic oxidation, the number of catalysts tested is still limited. Therefore, the establishment of a high throughput technical platform for catalyst screening would enhance the opportunity of discovering suitable catalysts for photo-degradation reaction. Formerly, Maier and co-workers [4], Suzuki and co-workers [12], and Matsumoto et al. [13] developed a high throughput technology for catalyst screening based on HPLC screening, PH imaging, and AFM, respectively. The bottleneck of these technologies is the low screening rate. To develop the technology further, screening methods of higher speed are needed. In this paper, we report the use of fluorescence photo-imaging method for catalyst screening, and the results obtained on the photo-degradation of 1,6-hexamethylenediamine over libraries of catalysts.

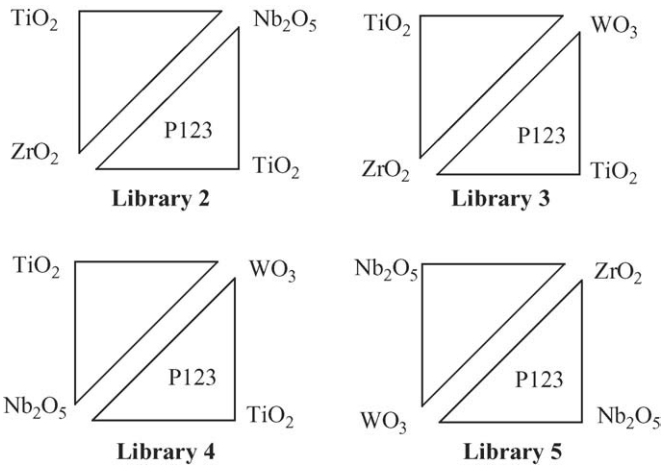

Fig. 1. The configuration of triangle sub-libraries.

2. Experimental

It was reported that by using P123 ($HO(CH_2CH_2O)_{20}(CH_2CH(CH_3)O)_{70}(CH_2CH_2O)_{20}H$, designated $EO_{20}PO_{70}EO_{20}$) as template, mesoporous materials of TiO_2, ZrO_2, Nb_2O_5, and WO_3 can be prepared [14].

In the synthesis of catalysts of Library 1, precursor solutions of $Mn(CH_3CO_2)_2$, $Fe(NO_3)_3$, NH_4F, $La(NO_3)_3$, $NaNO_2$, $Pb(NO_3)_2$, $AgNO_3$, NH_4Cl, $Mg(NO_3)_2$, $Co(NO_3)_2$, $Ni(NO_3)_2$, $Al(NO_3)_3$, $LiNO_3$, KOH, $Bi(NO_3)_3$, NH_4Br, $(NH_4)_5H_5[H_2(WO_4)_6]\cdot H_2O$, $Zn(NO_3)_2$, and $Ce(NO_3)_3$ were prepared by dissolving the individual compound in DI water. The concentration of each precursor solution was 0.10 M (based on metal cation, F^-, Cl^-, or Br^-). The precursor solution of $ZrCl_4$ or $NbCl_5$ was prepared by dissolving 1.16 or 1.35 g of the compound, respectively, in ethanol to make up a solution of 50 mL (Zr and Nb concentration should be 0.10 M).

In order to achieve high mechanical strength and for unambiguous interpretation of catalyst property, we used silica as support. With a specific surface area of 1.3 m^2/g, silica (<100 meshes) should not exert any significant influence on the chemical property of the catalysts. In a typical experiment, 10.0 g of SiO_2 was added to 20.0 mL of ethanol under vigorous stirring to generate a uniform suspension, and then 100 μL of the suspension was dispensed (still subject to vigorous stirring) to glass vessels (each 2.5 mL) that were arranged in array on an aluminum plate to form the blank silica library. To each glass vessel of blank silica library, 1000 μL of $TiCl_4$ precursor solution (prepared by dissolving 4.000 mL of $TiCl_4$ and 2.00 g of P123 in ethanol to make up a total volume of 80.0 mL) was dispensed to prepare the $TiCl_4$ precursor library. Then, 500 μL of a dopant solution was added to each glass vessel. The arrangement of the catalysts in Library 1 is shown in Table 1. As a reference, we prepared a TiO_2/SiO_2 catalyst in Library 1 without using P123. The precursor library was dried and hydrolyzed in air at 48 °C for 3 days, and then calcined at 450 °C for 5 h to obtain catalyst Library 1.

As shown in Fig. 1, four catalyst libraries were prepared. Each catalyst library contained two triangles of sub-libraries that contain catalysts of the same compositions at corresponding positions. In one of the two sub-libraries, the catalysts were prepared without P123, while in the other with P123.

In the preparation of "non-P123" sub-library catalysts in Libraries 2, 3, 4, and 5, Ti, Zr, and Nb precursor solutions were prepared by dissolving 3.80, 4.66, and 5.41 g of $TiCl_4$, $ZrCl_4$, and $NbCl_5$, respectively, in ethanol to make up a solution of 40.0 mL. The W precursor solution for non-P123 sub-library catalysts in Libraries 2–4 was different from that in Library 5. In the former cases, W precursor solution was prepared by adding 5.34 g of $(NH_4)_5H_5[H_2(WO_4)_6]\cdot H_2O$ (particle size < 100 mesh) in ethanol to prepare a 40.0 mL suspension under stirring, while in the latter case, the precursor solution was prepared by dissolving 3.96 g of WCl_6 in ethanol to make up a volume of 40.0 mL.

Table 1
The arrangement of catalysts of Library 1

$NH_4F/TiO_2(P123)/SiO_2$	$NH_4Cl/TiO_2(P123)/SiO_2$	$KOH/TiO_2(P123)/SiO_2$
$TiO_2(P123)/SiO_2$	$LiNO_3/TiO_2(P123)/SiO_2$	$NaNO_3/TiO_2(P123)/SiO_2$
$MgNO_3/TiO_2(P123)/SiO_2$	$Mn(NO_3)_2/TiO_2(P123)/SiO_2$	$Co(NO_3)_3/TiO_2(P123)/SiO_2$
$Pb(NO_3)_2/TiO_2(P123)/SiO_2$	$Al(NO_3)_3/TiO_2(P123)/SiO_2$	$NH_4Br/TiO_2(P123)/SiO_2$
$Fe(NO_3)_3/TiO_2(P123)/SiO_2$	$Ni(NO_3)_2/TiO_2(P123)/SiO_2$	$AgNO_3/TiO_2(P123)/SiO_2$
$Zn(NO_3)_2/TiO_2(P123)/SiO_2$	$Bi(NO_3)_3/TiO_2(P123)/SiO_2$	$Ce(NO_3)_3/TiO_2(P123)/SiO_2$
$La(NO_3)_3/TiO_2(P123)/SiO_2$	W[a]$/TiO_2(P123)/SiO_2$	$ZrCl_4/TiO_2(P123)/SiO_2$
$NbCl_5/TiO_2(P123)/SiO_2$		TiO_2/SiO_2 (reference, no. P123)

[metal]:[TiO_2] = 1:10, TiO_2 (wt):SiO_2 (wt) = 3:5, weight of SiO_2 = 0.050 g.
[a] W stands for $(NH_4)_5H_5[H_2(WO_4)_6]\cdot H_2O$.

Table 2
Catalyst ($LO_{n1}/MO_{n2}/NO_{n3}$) compositions in sub-libraries not counting silica (L, M, and N are metal ions, concentrations in mole)

MO_{n1}										NO_{n2}
100/0/0	90/10/0	80/20/0	70/30/0	60/40/0	50/50/0	40/60/0	30/70/0	20/80/0	10/90/0	0/100/0
90/0/10	80/10/10	70/20/10	60/30/10	50/40/10	40/50/10	30/60/10	20/70//10	10/80//10	0/90/10	
80/0/20	70/10/20	60/20/20	50/30/20	40/40/20	30/50/20	20/60/20	10/70//20	0/80/20/20		
70/0/30	60/10/30	50/20/30	40/30/30	30/40/30	20/50/30	10/60/30	0/70/30			
60/0/40	50/10/40	40/20/40	30/30/40	20/40/40	10/50/40	0/60/40				
50/0/50	40/10/50	30/20/50	20/30/50	10/40/50	0/50/50/50					
40/0/60	30/10/60	20/20/60	10/30/60	0/40/60						
30/0/70	20/10/70	10/20/70	0/30/70							
20/0/80	10/10/80	0/20/80								
10/0/9	0/10/90									
0/0/100										
LO_{n3}										

In the preparation of "P123" catalysts in the sub-libraries of Libraries 2–5, the Ti, Zr, and Nb precursor solutions were prepared by dissolving 1.00 g of P123 and 3.81 g of $TiCl_4$, 2.33 g of $ZrCl_4$, and 2.71 g of $NbCl_5$, respectively, in ethanol to make up a solution of 40.0 mL. The W precursor solution for Libraries 2–4 was prepared by adding 5.34 g of $(NH_4)_5H_5[H_2(WO_4)_6]\cdot H_2O$ (particle size <100 mesh) and 1.00 g of P123 in ethanol to prepare a 40.0 mL suspension under stirring, while that for Library 5 was prepared by dissolving 3.96 g of WCl_6 and 1.00 g of P123 in ethanol to make up a volume of 40.0 mL. Again, silica was used as support. To a SiO_2 triangle blank library, the as-prepared Ti, Zr, Nb, or W precursor solution was dispensed into the glass vessels, respectively, according to the concentration formula of Table 2 as well as the library configuration in Fig. 1. In each sub-library, there were 66 catalysts. The precursor libraries were then dried, hydrolyzed and calcined as mentioned before.

For the purpose of measuring the specific surface area, catalysts having the compositions of 50%ZrO_2-50%WO_3, 70%TiO_2-20%ZrO_2-10%WO_3, 20%TiO_2-10%ZrO_2-70%WO_3, 50%TiO_2-50%ZrO_2, 50%TiO_2-50%WO_3, 10%TiO_2-%ZrO_2-20%WO_3, and 40%TiO_2-30%ZrO_2-30%WO_3 were synthesized (in a scale of 0.50 g) according to the method described for the preparation of the catalysts in Library 3 by the use of P123, respectively (but without silica). Specific surface areas of catalysts were measured on a Beckman Coulter SA 3100 adsorption system. Nitrogen was used as an adsorbate. Before specific surface area measurement, the samples were evacuated to 3×10^{-5} Torr at 300 °C. The specific surface areas are listed in Table 3.

The activity evaluation of catalysts is based on a photo-fluorescence imaging technology. We chose 1,6-hexamethylenediamine, $NH_2(CH_2)_6NH_2$, as a probe molecule because a primary amine would react with fluorescamine to generate a substance that gives strong fluorescence light under UV irradiation (reaction (1)) [15].

The intensity of the fluorescence reflects the amount of 1,6-hexamethylenediamine present. The photocatalytic reaction is evaluated based on the removal of 1,6-hexamethylenediamine over the catalysts. The analysis was carried out on a home-built CCD-camera (WAT-525EX from WATEC) system (Fig. 2A). For catalyst screening, photocatalytic reactions were carried out over a 12×12 wells (10 mm ID, 15 mm depth) polytetrafluoroethylene (PTFE) reaction plate. The catalysts and 1,6-hexamethylenediamine (400 ppm by weight, 600 μL) were added to the wells, and placed in a lamp box (Fig. 2B, box dimensions 60 cm × 60 cm × 60 cm). There were six medium pressure mercury UV lamps (each 15 W) on the ceiling of the box. The intensity of UV irradiation (254 nm) at the library position was 233 $\mu W/cm^2$. After recording the initial data, the reaction plate was placed under UV irradiation, and samples were drawn for fluorescence imaging at various stages of reaction.

During the analysis, a picture of the PTFE detection plate (with 14×14 wells, well diameter 4.0 mm, depth 3.0 mm) was taken as background (Fig. 3, Picture A). After the catalysts and 1,6-hexamethylenediamine aqueous solution were transferred to the reaction plate and kept in darkness for 20 min (to reach adsorption–desorption equilibrium), 30 μL of 1,6-hexamethylenediamine aqueous solution was transferred from each of the wells on the reaction plate to the corresponding wells of the detection plate, and then 30 μL of fluorescamine DMF (*N*,*N*-dimethyl formate) solution (800 ppm by weight) was added into each of the wells of the detection plate. After 10 min, a picture was taken (denoted as Picture B). Picture B stands for the starting point of the reaction. After photocatalytic reaction, 30 μL of aqueous solution from individual sample well of the reaction plate (Fig. 2B) was transferred to the corresponding well of the detection plate, and then 30 μL of fluorescamine DMF solution (800 ppm by weight) was added, respectively, into the wells of detection

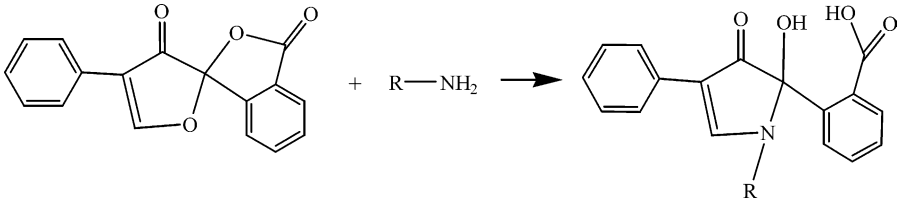

(1)

Table 3
The specific surface area and pore size of catalysts prepared with (A) or without (B) P123 template

Catalyst	S_{BET} (m^2/g)	Pore diameter (nm)	Catalyst	S_{BET} (m^2/g)	Pore diameter (nm)
TiO_2(A)	78.8	3.65–20	TiO_2(B)	44.1	–
ZrO_2(A)	68.3	3.65	ZrO_2(B)	49.8	–
Nb_2O_5(A)	111.4	3.65	Nb_2O_5(B)	8.33	–
WO_3(A)	19.4	36.57	WO_3(B)	15.3	–
70%TiO_2-20%ZrO_2-10%WO_3(A)	79.8	10.0	50%ZrO_2-50%WO_3(A)	16.8	30.2
20%TiO_2-10%ZrO_2-70%WO_3(A)	54.7	16.0	50%TiO_2-50%ZrO_2(A)	64.2	–
10%TiO_2-70%ZrO_2-20%WO_3(A)	78.2	5.8	50%TiO_2-50%WO_3(A)	70.3	5.8
40%TiO_2-30%ZrO_2-30%WO_3(A)	77.3	12.3			

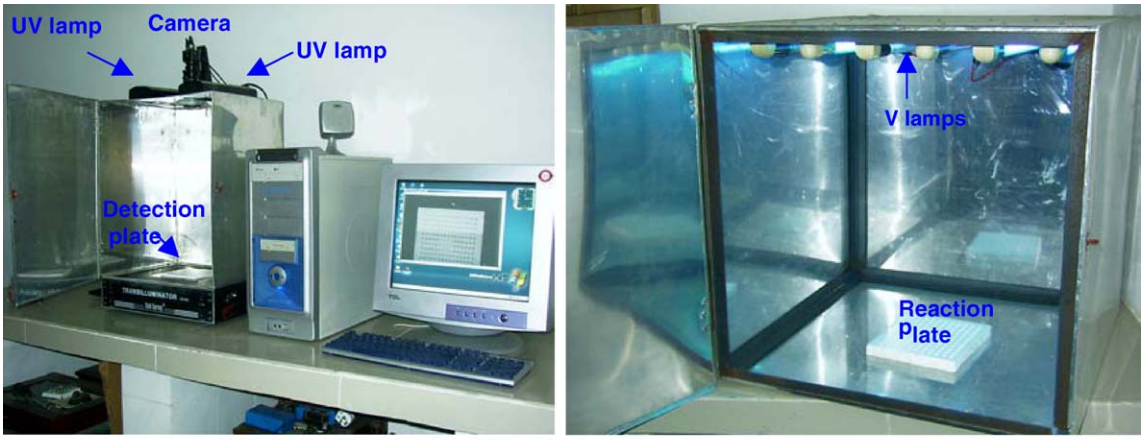

Fig. 2. Photos of (A) fluorescence imaging system and (B) photocatalytic reactor.

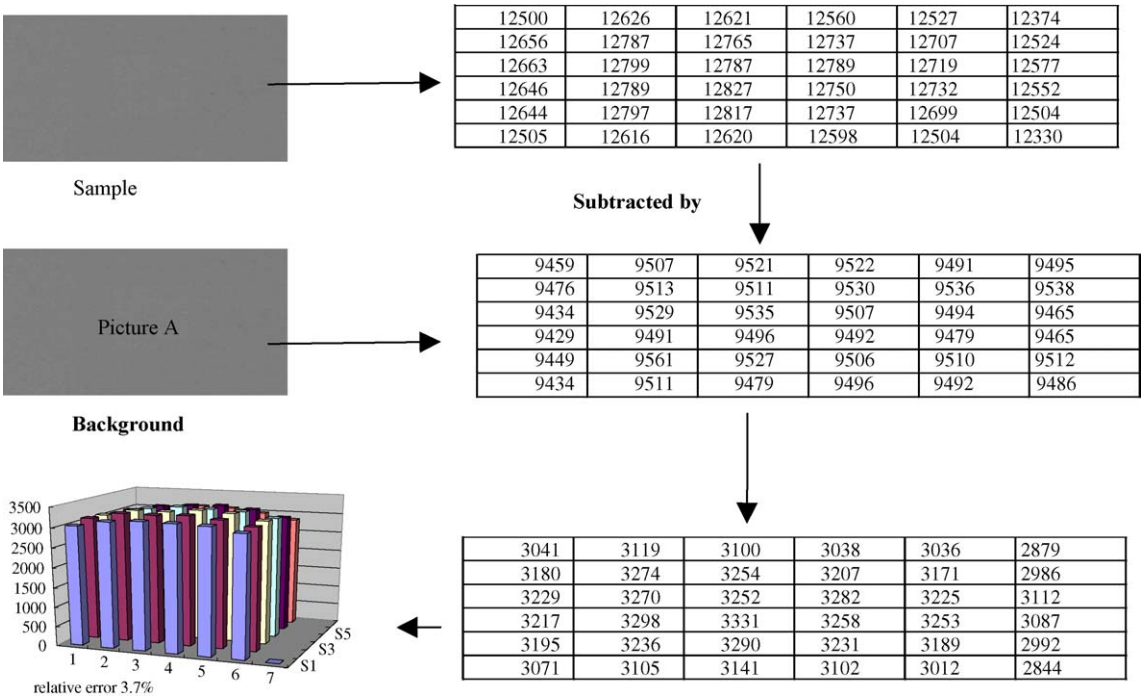

Fig. 3. The flow chart of data reduction.

plate. After 10 min, another picture was taken (denoted as Picture C) to reflect the consumed amount of 1,6-hexamethylenediamine. The samples appeared on the picture as light-up spots. A program (IMGI) developed by us was used to convert the intensities of light-up spots to numerical values. The number (defined as appearance conversion, X) obtained as a result of dividing the difference between each corresponding datum of Picture B and that of Picture C by the difference between that of Picture B and that of Picture A would provide information related to the consumption amount of 1,6-hexamethylenediamine. The data flow sheet is shown in Fig. 3. Despite the fact that fluorescence response to 1,6-hexamethylenediamine conversion is not linear, the results are adequate to differentiating the good catalysts from the poor ones. The control experiment was carried out by mixing 1,6-hexamethylenediamine (30 μL, 400 ppm) with fluorescamine solution in DMF (30 μL, 800 ppm) in the wells of the detection plate. Separately, a 6 × 6-element library was generated and analyzed to evaluate the relative error of the analytical approach. The results indicate a relative error of 3.7%. Taking the catalyst influences and other effects into account, the overall relative error was estimated to be below 6%.

Methyl orange is commonly used as a reactant for the evaluation of photo-degradation activity [10,16]. For comparison, we used aqueous solutions of both 1,6-hexamethylenediamine and methyl orange as reactants, respectively, over TiO_2, WO_3, and Nb_2O_5. In the former case, 600 μL of 1,6-hexamethylenediamine aqueous solution (400 ppm) and 30.0 mg of catalyst were mixed, and the reactions were carried out in the PTFE reaction plate without stirring. In the latter case, 7.0 mL of methyl orange aqueous solution (16.7 ppm by weight) and 0.500 g of catalyst were used, and the reaction was carried out in a glass beaker with a bottom area of 9.1 cm^2; the catalyst was settled to cover the bottom of the beaker and the reaction was carried out without stirring. After the reaction, the former case was handled with the fluorescence method, while the latter was analyzed by using a UV spectrophotometer (Shang Hai Analysis Instrument Inc.). For the observation of the activities over the non-TiO_2 catalysts, the WO_3, Nb_2O_5, 30%WO_3-10%Nb_2O_5-60%ZrO_2, and 40%Nb_2O_5-10%ZrO_2-50%WO_3 catalysts selected from Library 5, and 80%TiO_2-20%WO_3 and 80%TiO_2-20%ZrO_2 catalysts selected from Libraries 3 and 4 were evaluated by using methyl orange as the reactant. XRD examination of catalysts was also performed over a Philips PW3040/60 X-ray diffraction spectrometer with Cu Kα irradiation.

3. Results and discussion

3.1. Physical properties

In this research work, we intend to synthesize catalysts of high specific surface area in catalyst libraries containing TiO_2, ZrO_2, Nb_2O_5, and WO_3 as well as their mixtures prepared by using P123. With hundreds of catalysts, it is impracticable to measure the BET surface area of each individual one. As a compromise, we checked certain catalysts to see if they have large specific surface area when P123 was used as template. Hence,

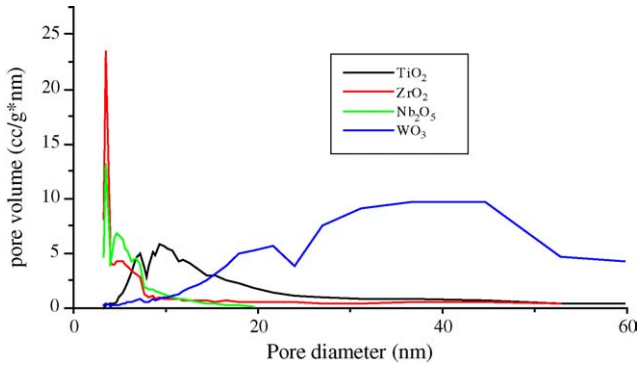

Fig. 4. The pore diameter distribution of TiO_2, ZrO_2, Nb_2O_5, and WO_3 prepared by using P123 as template.

only 50%ZrO_2-50%WO_3, 70%TiO_2-20%ZrO_2-10%WO_3, 20%TiO_2-10%ZrO_2-70%WO_3, 50%TiO_2-50%ZrO_2, 50%TiO_2-50%WO_3, 10%TiO_2-70%ZrO_2-20%WO_3, and 40%TiO_2-30%ZrO_2-30%WO_3 catalysts of Library 3 were scaled up and their specific surface areas and pore diameter distribution were measured. Table 3 indicates that besides 50%TiO_2-50%ZrO_2, the other binary and tertiary materials are mesoporous, large in specific surface areas and uniform in pore structure.

The materials TiO_2, ZrO_2, and Nb_2O_5 prepared by using P123 as template are mesoporous, and have relatively high in specific surface area (Table 3). As revealed by the results of Fig. 4, ZrO_2 and Nb_2O_5 show high pore-size uniformity (diameter 3.65 nm), while TiO_2 shows low pore-size uniformity (from 3.65 to 20 nm). The TiO_2, ZrO_2, and Nb_2O_5 materials prepared without P123 are not mesoporous, and are relatively small in specific surface area. The WO_3 material is not mesoporous no matter it is prepared by P123 or not, and the specific surface area is small.

3.2. Methyl orange and 1,6-hexamethylenediamine as reactants

As described in Section 2, methyl orange was used as a reactant to evaluate the adopted photo-fluorescence analytical method. Shown in Fig. 5 are the results obtained after 4 h of UV irradiation. The data serial (a) was obtained by using methyl orange (in aqueous solution) as a reactant and the consumption numbers of methyl orange over TiO_2, WO_3, and Nb_2O_5 were calculated based on UV spectrometric analysis. The data serial (b) was obtained by using 1,6-hexamethylenediamine (in aqueous solution) as reactant and calculated based on the results of photo-fluorescence analysis. Fig. 5 indicates that the variation trends of X_i number over TiO_2, WO_3, and Nb_2O_5 are the same. Among TiO_2, WO_3, and Nb_2O_5, TiO_2 was the most active, and Nb_2O_5 the second most active for 1,6-hexamethylenediamine or methyl orange photo-degradation. The results indicate that both UV and the photo-fluorescence analyses can make a differentiation between good and poor catalysts.

3.3. Library 1

When 1,6-hexamethylenediame in aqueous solution was subjected to two hours of UV irradiation, the TiO_2 catalyst prepared

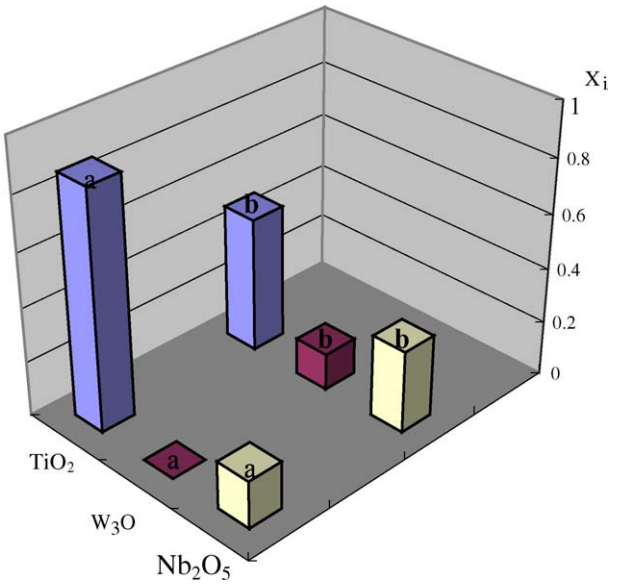

Fig. 5. Data of serial (a) and (b) (please refer to text for illustration).

by using P123 was more active than the one prepared without P123 (Fig. 6). It is apparent that the TiO_2 catalyst with higher specific surface area was more active than that with lower specific surface area. As shown in Fig. 6, the Cl^--, Br^--, Ag-, or WO_3-doped TiO_2 catalysts are significantly higher than pure TiO_2 (not counting SiO_2) in activity. For ZrO_2-doped TiO_2, experimental reproducibility was rather poor, sometimes ZrO_2-doping improved the catalytic activity but sometimes did not. We deduce that in the case of ZrO_2-doping, catalytic properties might be sensitive to catalyst preparation procedure. The F^--, Na^+-, or CeO_2-doped TiO_2 catalysts show activity similar to that of pure TiO_2. Except the above-mentioned catalysts, those prepared by doping TiO_2 with the other dopants (as listed in Table 1) showed lower activity than pure TiO_2. During catalyst preparation, Cl^- and Br^- were removed from the catalysts and should not influence the catalytic activity of TiO_2. However, if Cl^- and Br^- influence the crystallization process of components in catalysts, the catalytic properties might change as a result.

It was reported that doping TiO_2 with Ag would result in activity improvement [17], and the upper limit of Ag loading was 2%. In our case, Ag loading was about 9.1%, far above the reported upper limit. However, the 9.1%Ag/TiO_2 catalyst showed higher activity than pure TiO_2. Our study also revealed that if TiO_2 were prepared without using P123, doping TiO_2 (44.1 m^2/g) with 9.1% Ag would lead to a decrease in activity. We believe that in the case of Library 1, the TiO_2 catalyst prepared by P123 has a specific surface area of 78.8 m^2/g, nearly double that (44.1 m^2/g) of the TiO_2 prepared without P123; the Ag could spread out much better on the larger surface. Lee et al. found that the photocatalytic activity of WO_3/TiO_2 film is 2.8–3.0 times that of pure TiO_2 film in decomposing gas-phase 2-propanol, while MoO_3/TiO_2 film is less effective [18]. Although we did not observe such a large increase in catalytic activity after doping TiO_2 with WO_3, we observed a clear increase in catalytic activity in the WO_3-doped case.

3.4. Library 2

In Library 2, two sub-libraries of Zr-Ti-Nb-O catalysts were present. The results obtained after 2 h of UV irradiation are shown in Fig. 7. In both cases of with and without P123, pure TiO_2 showed higher activity than pure Nb_2O_5 and ZrO_2, consistent with the fact that TiO_2 is a well-documented photodegradation catalyst. With P123 being template, the Nb_2O_5-doped TiO_2 catalysts showed the highest catalytic activity. The best concentration of Nb_2O_5 in TiO_2 is 30–50% (atomic mole). It is apparent that ZrO_2-doping did not have any significant effect on TiO_2 catalytic activity. The results suggest that ZrO_2-doping might not be good for Nb_2O_5-TiO_2 catalysts.

In the set of catalysts prepared without P123 template, ZrO_2-doped TiO_2 showed higher catalytic activity in the ZrO_2 concentration range of 20–80%. For the TiO_2-ZrO_2 binary catalysts, our study showed poor reproducibility. The Nb_2O_5-doped cat-

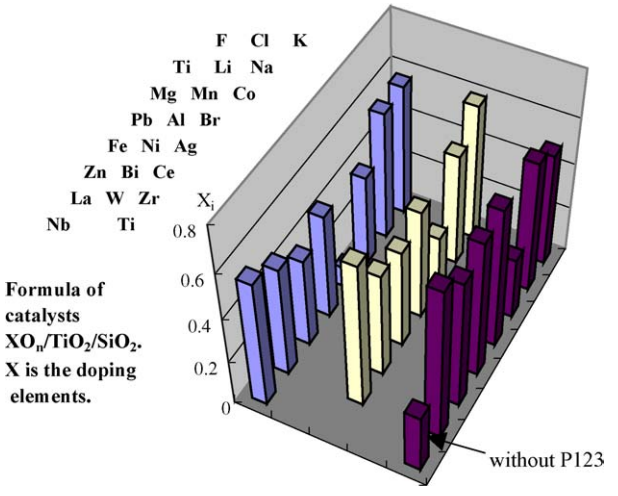

Fig. 6. Performance of catalysts in Library 1 (please refer to the left top corner for the array of elements, [X]:[TiO_2] = 1:10, TiO_2 (wt):SiO_2 (wt) = 3:5, weight of SiO_2 = 0.050 g.

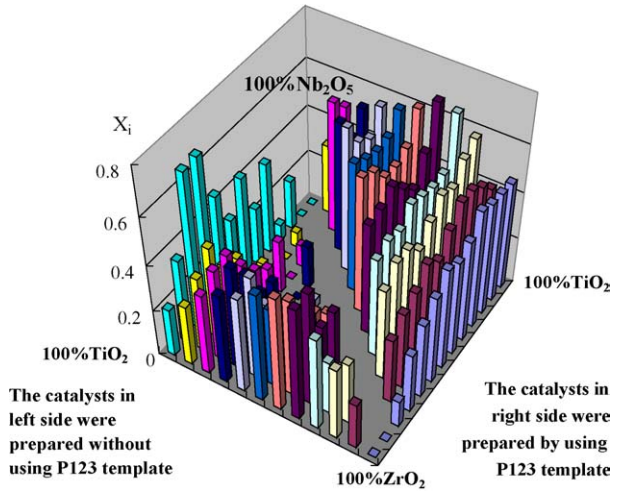

Fig. 7. Performance of catalysts (please refer to Table 2 for catalyst compositions, not counting silica) in Library 2.

alysts showed the highest catalytic activities with Nb concentrations ranging from 30 to 50%, and the activities were almost the same as those of the Nb_2O_5-TiO_2 catalysts prepared via P123 template within the same Nb_2O_5 concentration range. As found in Library 1, when Nb doping concentration was 9.1% in the Nb-Ti-O catalyst, the catalyst did not show higher activity higher than pure TiO_2 (Fig. 6). Comparing the results of Libraries 1 and 2, one would conclude that in the case of Library 1, a doping concentration of 9.1% Nb_2O_5 does not improve the catalytic activity of TiO_2. Again, without P123 as template, the ZrO_2-doped Nb_2O_5-TiO_2 catalysts did not show any improvement in catalytic performance. Comparing the results of the two sub-libraries, we found that except the most active Nb_2O_5-TiO_2 catalysts, most of the other catalysts prepared with P123 template were more active than those prepared without P123.

3.5. Library 3

In catalyst Library 3, two ZrO_2-TiO_2-WO_3 sub-libraries were present. After 2 h of UV irradiation, the consumption of 1,6-hexamethylenediamine over the catalysts are shown in Fig. 8. Among the pure ZrO_2, TiO_2, and WO_3 in the two sub-libraries, TiO_2 showed the highest activity, consistent with that observed over catalyst Library 2. The doping TiO_2 with ZrO_2 did not have any positive effects on catalytic activities no matter whether the catalyst was prepared with or without P123. This is not consistent with that observed over Library 2 where ZrO_2 showed positive effect on TiO_2 activity when without P123. Also, the results indicated that ZrO_2-doping did not have any positive effect on the catalytic activity of WO_3-TiO_2 catalysts. However, doping TiO_2-ZrO_2 with WO_3 led to an apparent increase in activity; when WO_3 concentration was 10% in TiO_2-ZrO_2-WO_3 catalysts, the catalysts showed higher activity than TiO_2-ZrO_2 catalysts. Irrespective of whether prepared with or without P123 template, the WO_3-TiO_2 catalysts showed the best activities. When prepared via P123 template, the WO_3-TiO_2 catalyst with

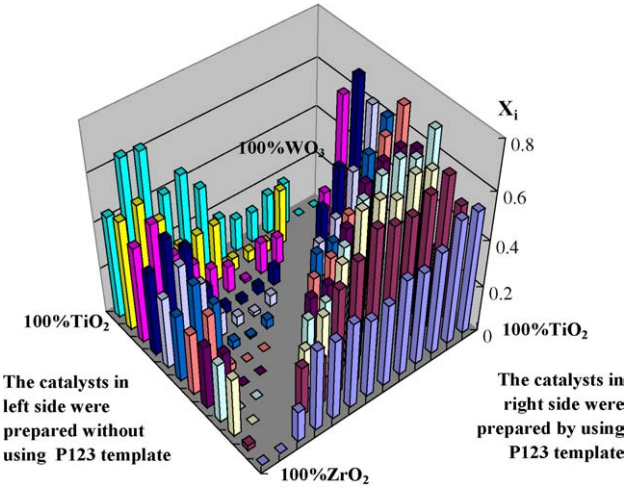

Fig. 8. Performance of catalysts (please refer to Table 2 for compositions of catalysts) in Library 3.

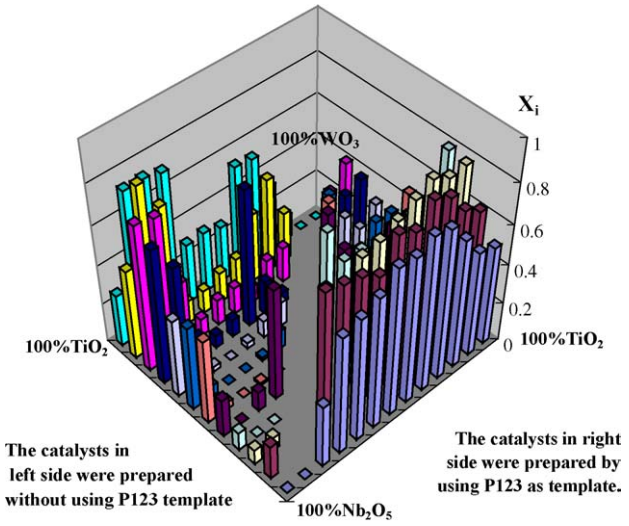

Fig. 9. Performance of catalysts (please refer to Table 2 for catalyst compositions) in Library 4.

WO_3 concentration from 30 to 50% showed high catalytic activities. When there was no involvement of P123, the WO_3-TiO_2 catalysts with WO_3 concentration of 10–30% showed the best catalytic activities. Also, WO_3 showed positive effect on the catalytic activity of ZrO_2-TiO_2 catalysts containing 0–70% ZrO_2. The catalysts prepared with P123 are more active than that prepared without it.

3.6. Library 4

In Libraries 2 and 3, we found that Nb_2O_5- or WO_3-doped TiO_2 catalysts showed high activity. In order to finding out if there were co-doping effects of Nb_2O_5 and WO_3 on TiO_2, we examined two WO_3-TiO_2-Nb_2O_5 sub-libraries. In one of the sub-libraries, catalysts were synthesized by using P123 as template, while the catalysts in the other was without it. Shown in Fig. 9 are the catalytic activities in 2 h of UV irradiation. In both sub-libraries, TiO_2 showed higher catalytic activity than WO_3 and Nb_2O_5, being consistent with those obtained in Libraries 2 and 3. Without P123 template for the preparation of WO_3-TiO_2 binary catalysts, catalysts containing 10–30% of WO_3 showed the highest catalytic activities. For Nb_2O_5-TiO_2 binary catalysts, when Nb_2O_5 concentration was from 20 to 30%, the catalysts showed the best activities. In this case, WO_3 and Nb_2O_5 showed positive co-doping effect on TiO_2 catalyst. We found that 10%WO_3-10%Nb_2O_5-80%TiO_2 was the most active catalyst in the sub-library without P123.

Prepared with P123, the WO_3-TiO_2 binary catalysts containing 20–30% of WO_3 had the highest catalytic activities. Among the Nb_2O_5-TiO_2 binary catalysts, the catalysts containing 20–60% of Nb_2O_5 were very active. In this sub-library, WO_3 and Nb_2O_5 showed strong positive co-doping effects on the catalytic activity of TiO_2. When the catalyst contained 20–30% of Nb_2O_5 and 10–20% of WO_3 (balanced by TiO_2), the WO_3-Nb_2O_5-TiO_2 catalysts showed the highest catalytic activity in the library. Comparing the catalysts of the two sub-libraries, we found that with or without P123, the “most active” catalysts

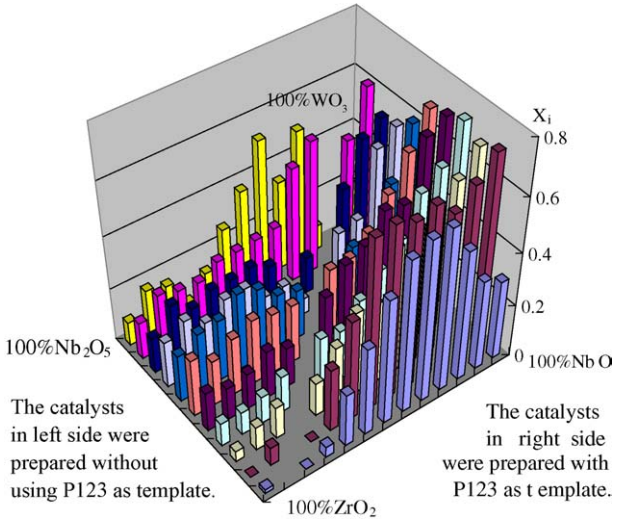

Fig. 10. Performance of catalysts (please refer to Table 2 for catalyst compositions) in Library 5.

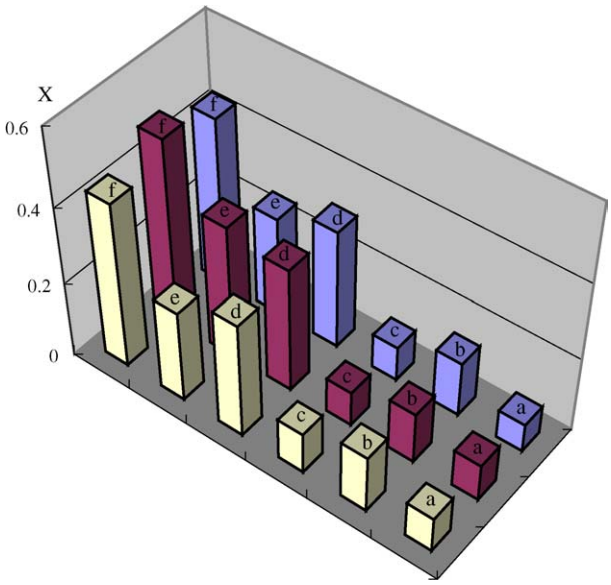

Fig. 11. Performance of catalysts with compositions: (a) WO_3, (b) Nb_2O_5, (c) 30%WO_3-10%Nb_2O_5-60%ZrO_2, (d) 80%TiO_2-20%WO_3, (e) 80%TiO_2-20%ZrO_2, and (f) 40%Nb_2O_5-10%ZrO_2-50%WO_3 by using methyl orange as reactant (three runs for each catalyst).

actually showed similar catalytic activities. However, for the rest of the catalysts, the catalysts prepared with P123 template showed much higher activity than those prepared without it.

3.7. Library 5

In Library 5, no catalyst contained TiO_2. The WO_3-Nb_2O_5-ZrO_2 catalysts in two sub-libraries were screened. The results obtained after two hours of UV irradiation are shown in Fig. 10. In the case of catalysts prepared without P123, pure WO_3, Nb_2O_5, and ZrO_2 did not exhibit high catalytic activities. Among the ZrO_2-Nb_2O_5 binary catalysts, the most active one was found to contain 50% of ZrO_2. However, the ZrO_2-Nb_2O_5 binary catalysts did not show high activity, even the most active one (50%ZrO_2/Nb_2O_5) did not exhibit good activity (X_i is below 0.20). Among the WO_3-ZrO_2 binary catalysts, only the one containing 90% of WO_3 showed high activity ($X_i = 0.50$). Among the WO_3-Nb_2O_5 binary catalysts, the catalysts containing 70–90% of WO_3 showed high activities. All the highly active catalysts were found to have high WO_3 concentration (10–40%Nb_2O_5/10%ZrO_2/50–80%WO_3).

We found that most of the catalysts prepared by using P123 as template showed higher activities than those prepared without it (Fig. 10). In this case, pure WO_3, Nb_2O_5, and ZrO_2 still did not show good activities (Nb_2O_5 X_i of 0.30 is the highest among WO_3, Nb_2O_5, and ZrO_2.). Among the ZrO_2-Nb_2O_5 binary catalysts, the catalysts containing 30–40% of ZrO_2 exhibit high activities (X_i reached 0.61). The results are consistent with those obtained in Library 2 (Fig. 7). Among the WO_3-ZrO_2 binary catalysts, the catalysts containing 90% WO_3 showed good activity, which is consistent with the results obtained in sub-library prepared without P123, and that of Library 3 with P123 (Fig. 8). Among the WO_3-Nb_2O_5 binary catalysts, the catalysts containing 30–40% of WO_3 showed high activities, which is consistent with the results obtained in catalyst Library 4 (Fig. 9). The results indicate that with WO_3 addition to ZrO_2-Nb_2O_5 reaching a WO_3 concentration of about 10%, there was improvement in catalytic activity. However, the most active catalyst was found among the WO_3-Nb_2O_5 binary catalysts, which contained 30–40% of WO_3. The doping of ZrO_2 in WO_3-Nb_2O_5 binary catalysts did not show apparent effect on catalytic activity.

When methyl orange was used as a reactant, the results compiled in Fig. 11 were obtained. The WO_3, Nb_2O_5, 30%WO_3-10%Nb_2O_5-60%ZrO_2, and 40%Nb_2O_5-10%ZrO_2-50%WO_3 catalysts were selected from catalyst Libraries 3–5. The catalysts WO_3, Nb_2O_5, and 30%WO_3-10%Nb_2O_5-60%ZrO_2 are not active whereas 40%Nb_2O_5-10%ZrO_2-50%WO_3 is active (Fig. 10). It can be seen that the activity variation trend in Fig. 11 is consistent with that observed in Library 5. Catalyst 80%TiO_2-20%WO_3 was active and was more active than 80%TiO_2-20%ZrO_2 (Fig. 8); we observed a similar trend in Fig. 11. Similarly, we confirmed that 40%Nb_2O_5-10%ZrO_2-50%WO_3 is more active than 80%TiO_2-20%WO_3 (Figs. 9 and 11). The results obtained by using methyl orange as a reactant and UV spectrometric analysis are consistent with those obtained by using 1,6-hexmethylenediamine as a reactant and fluorescence photo-imaging as the analysis method.

In order to gain insight into the nature of the active "non-TiO_2" catalysts, we selected catalysts WO_3-Nb_2O_5, Nb_2O_5-ZrO_2, and WO_3-ZrO_2 with a metal atomic ratio of 1:1 prepared with P123 as template from Library 5, and performed XRD investigation (Fig. 12). In Library 5, WO_3-Nb_2O_5 is more active than Nb_2O_5-ZrO_2 and WO_3-ZrO_2. The XRD results showed that both Nb_2O_5-ZrO_2 and WO_3-ZrO_2 are amorphous materials; it is not possible to identify any phase structures. As in the case of WO_3-Nb_2O_5, Nb_2O_5, and $H_3ONb_3O_8$ phases were detected whereas no WO_3 phases were observed. It is possible that there was W^{6+} incorporation into the Nb_2O_5 and $H_3ONb_3O_8$ lattices without much structural distortion. There are two ways of maintaining electro-neutrality within the materials. One is having

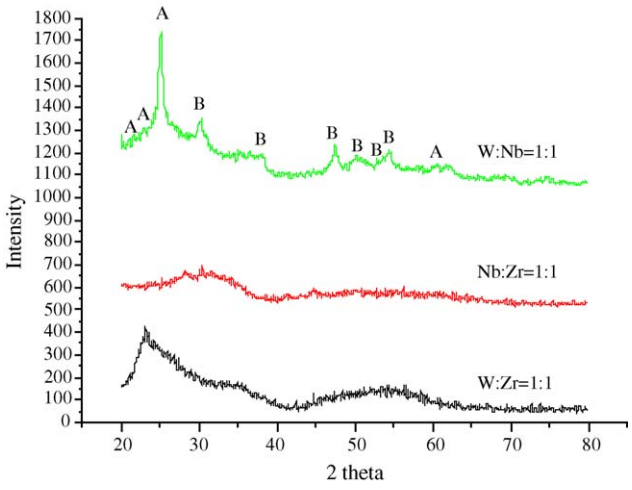

Fig. 12. XRD of the samples WO_3-ZrO_2, Nb_2O_5-ZrO_2, and WO_3-Nb_2O_5 with metal atomic ratio of 1:1 (B) Nb_2O_5, (A) $H_3ONb_3O_8$.

equivalent amount of O^{2-} anions around the W^{6+} ions in the interstitial positions; the other is having cation vacancies created inside the lattice structures. We suggest that both situations could have had occurred. We observed that under UV or visible light irradiation and in the absence of oxygen or air, the yellow WO_3-Nb_2O_5 catalysts with WO_3 concentrations ranging from 10 to 50% turned blue (a signal of W^{5+} formation). With the removal of the light sources, the stable blue color changed back to yellow if the materials were exposed to oxygen or air. It is known that the bandgap energy of WO_3 is 2.8 eV, small enough to allow photo-activity under even visible light ($\lambda < 443$ nm). However, pure WO_3 does not show any significant activity in photo-degradation reactions, plausibly due to the fast recombination rate of the electron-hole pairs inside pure WO_3. When WO_3 was incorporated into the Nb_2O_5 and $H_3ONb_3O_8$ lattices and with the trapping of an electron, W^{6+} turned to W^{5+}. The stable blue color of WO_3-Nb_2O_5 under UV or visible light irradiation indicates that with W^{5+} ions carrying the same charge as Nb^{5+} ions, the photo electron–hole pairs in the Nb_2O_5 and $H_3ONb_3O_8$ lattices are stabilized. Further experiments are being conducted in our laboratory for the verification of such an explanation for the photocatalytic activity observed over the newly found catalysts.

4. Conclusion

By using P123 as template, we prepared mesoporous TiO_2, ZrO_2, Nb_2O_5, and WO_3, as well as the "P123" catalysts in the catalyst libraries, such as 50%ZrO_2-50%WO_3, 70%TiO_2-20%ZrO_2-10%WO_3, 20%TiO_2-10%ZrO_2-70%WO_3, 50%TiO_2-50%WO_3, 10%TiO_2-70%ZrO_2-20%WO_3, and 40%TiO_2-30%ZrO_2-30%WO_3. In the control experiments, the results obtained by using 1,6-hexamethylenediamine as a reactant and adopting the fluorescence photo-imaging approach were comparable to those obtained by using methyl orange as reactant and UV spectrophotometer as analytical device. The mesoporous catalysts of high specific surface area are higher in catalytic activities than the "non-P123" catalyst materials in photo-degradation of 1,6-hexamethylenediamine. The investigation also revealed that ZrO_2-doping to TiO_2 resulted in no improvement, whereas doping TiO_2 with Nb_2O_5 or WO_3 enhanced the catalytic activities, and the co-doping of Nb_2O_5 and WO_3 to TiO_2 showed strong positive effect on catalytic performance. The catalysts (WO_3-Nb_2O_5-TiO_2) containing 20–30% Nb_2O_5 and 10–20% WO_3 (balanced by TiO_2) showed activities higher than any of TiO_2, Nb_2O_5, WO_3, and the binary catalysts composed of any two of TiO_2, Nb_2O_5, and WO_3. Our study also showed that beside the traditional TiO_2-domain catalysts, very active photo-degradation catalysts could be prepared via the combinations of Nb_2O_5, WO_3, and ZrO_2. It means that by adopting suitable high throughput tools and with the knowledge of catalytic chemistry, there is a high chance of discovering good catalysts other than those of TiO_2-domain ones.

Acknowledgments

We thank the Nature Science Foundation of China for financial support (Project No. 20277008) and the National Analysis Key Laboratory of Hunan University for instrument support. C.T.A. thanks the Hunan University for an adjunct professorship.

References

[1] M.R. Hoffmann, S.T. Martin, W.Y. Choi, D.W. Bahnemann, Chem. Rev. 95 (1995) 69.
[2] C.Y. Wang, D.W. Bahnemann, J.K. Dohrmann, J. Chem. Soc., Chem. Commun. (2000) 1539.
[3] A. Mills, S.L. Hunte, J. Photochem. Photobiol. A: Chem. 108 (1997) 1.
[4] C. Lettmann, H. Hinrichs, W.F. Maier, Angew. Chem. Int. Ed. 40 (2001) 3160.
[5] L. Cao, A. Huang, F.J. Spiess, S.L. Suib, J. Catal. 188 (1999) 48.
[6] A.J. Maira, K.L. Yeung, C.Y. Yan, P.L. Yue, C.K. Chan, J. Catal. 192 (2000) 185.
[7] A.J. Maira, K.L. Yeung, J. Soria, J.M. Coronado, C. Belver, C.Y. Lee, V. Augugliaro, Appl. Catal. B: Environ. 29 (2001) 327.
[8] I. Ilisz, A. Dombi, K. Mogyorósi, I. Dékány, Colloids Surf. A: Physicochem. Eng. Aspects 230 (2004) 89.
[9] R.J. Berry, M.R. Mueller, Microchem. J. 50 (1994) 28.
[10] X.H. Liu, C.X. Liang, H.Z. Wang, X.J. Yang, L. Lu, X. Wang, Mater. Sci. Eng. A 326 (2002) 235.
[11] D.W. Bahnemann, S.N. Kholuiskaya, R. Dillert, A.I. Kulak, A.I. Kokorin, Appl. Catal. B: Environ. 36 (2002) 161.
[12] A. Nakayama, E. Suzuki, T. Ohmori, Appl. Surf. Sci. 189 (2002) 260.
[13] Y. Matsumoto, T. Ohsawa, K. Nakajima, H. Koinuma, Meas. Sci. Technol. 16 (2005) 199.
[14] P.D. Yang, D.Y. Zhao, D.I. Margolese, B.F. Chmelka, G.D. Stucky, Nature 396 (1998) 152.
[15] P.J. Desrosiers, C.E. Dube, X.P. Zhou, WO Patent 0014529 A1. (2000).
[16] C. Baiocchi, M.C. Brussino, E. Pramauro, A.B. Prevot, L. Palmisano, G. Marci, Int. J. Mass Spectrom. 214 (2002) 247.
[17] H. Tsuji, H. Sugahara, Y. Gotoh, J. Ishikawa, Nucl. Instrum. Methods Phys. Res. B 206 (2003) 249.
[18] K.Y. Song, M.K. Park, Y.T. Kwon, H.W. Lee, W.J. Chung, W.I. Lee, Chem. Mater. 13 (2001) 2349.